

doi:10.15199/48.2024.05.36

## Stationary thermal field in the direct current gas-insulated line

**Abstract.** The paper has analyzed a stationary thermal field in a direct current gas-insulated line (DC GIL). After assuming some simplifications, a mathematical model for the system is the boundary problem of the Poisson equation. The conditions of continuity of temperature and heat flux increments were assumed at the boundaries of material layers. The cooling of the system was modelled using Hankel's condition (of the 3rd kind) with the total heat transfer coefficient (i.e. with the sum of the convective and the radiation coefficients). The problem was solved analytically. After tabulating the formulas, the respective distributions were shown graphically. Additionally, the steady-state current rating was determined. The obtained results have a very good physical interpretation.

**Streszczenie.** W artykule analizowano stacjonarne pole termiczne w izolowanej gazem linii prądu stałego (DC GIL). Po przyjęciu odpowiednich uproszczeń, matematycznym modelem układu jest brzegowe zagadnienie równania Poissona. Na granicach stref materiałowych założono warunki ciągłości przyrostów temperatury i strumieni cieplnych. Chłodzenie układu modelowano za pomocą warunku Hankela (III rodzaju) z całkowitym współczynnikiem przejmowania ciepła (tzn. z sumą współczynników konwekcyjnego i radiacyjnego). Zagadnienie rozwiązano na drodze analitycznej. Po stabilizowaniu wzorów, odpowiednie rozkłady przedstawiono w postaci graficznej. Dodatkowo wyznaczono dopuszczalny prąd długotrwały. Otrzymane wyniki posiadają bardzo dobrą interpretację fizyczną. (Stacjonarne pole termiczne w izolowanej gazem linii prądu stałego (DC GIL)).

**Keywords:** direct current gas-insulated line (DC GIL), stationary thermal field, Poisson's equation boundary problem, steady state current rating

**Słowa kluczowe:** izolowana gazem linia prądu stałego (DC GIL), stacjonarne pole termiczne, brzegowe zagadnienie równania Poissona, dopuszczalny prąd długotrwały.

### Introduction

Gas-insulated lines are widely used in contemporary electrical engineering. This is due to the substantial advantages of this type of systems. From among them, the following can be mentioned: high working reliability, low operation costs, and straightforward construction and assembly. Moreover, no insulating oil is required in the device. In parallel with the widespread alternating current gas-insulated lines, AC GIL, also direct current gas-insulated lines (DC GIL) have been used for some time now [1], [2]. Their main advantages include: very low power losses over long distances, no variable electromagnetic field and thus the absence of any additional heat sources in the metal enclosure, and high current throughput. DC GILs are environmentally friendly.

One of the basic operating parameters of gas-insulated lines is the system's temperature. It is decisive to the system's reliability. For example, overheating can be the cause of a damage to the stand-off insulators, the power connection or the enclosure insulation. The temperature affects also the mechanical resilience, corrosion and oxidation of metallic parts and the quality and strength of butt joints. As the temperature is generated mainly by the flow of current, the above-mentioned deficiencies reduce the system's value. For the reasons given above, the thermal analysis of the system's field is an important technical task.

Thermal analysis of gas-insulated system has been the subject of few studies. In article [3], the analytical thermal balance method was employed for determining the temperature of conductors and enclosures in a three-phase alternating current GIL system. It was assumed that the system gave up heat to the environment by convection and radiation. The obtained results were verified by the finite element method and with laboratory measurements. In article [4], the increment in the temperature of an extra-high voltage gas-insulated switchgear bus bar was calculated. The thermal field was generated by power losses. The latter were determined by making the analysis of the electromagnetic field numerically (by the finite element method). The convention model of heat exchange was

assumed. A similar approach was presented in works [5],[6], where coupled magnetothermal analyses were performed. In [7], the thermal field generated by alternating current in three-phase GIL systems was examined using analytical and numerical methods. The aforementioned studies were limited to metallic enclosures not coated with insulation. The above literature review shows that no thermal analyses have been published for gas-insulated direct current systems and that the additional insulation on the metallic enclosure has not been considered. In the present paper, the equivalent thermal conduction coefficient has been employed to consider convective and radiative heat transfer in a cylindrical slot containing gas [8],[9],[10]. Such an approach substantially facilitates the analysis of the thermal field in systems with their volumes being partially filled with gas. In that case, the classical heat equation can be used.

### Physical and Mathematical Model of the DC GIL System

The subject of analysis is a DC gas-insulated line model consisting of four distinguished zones (Fig. 1) [11]. In the zone designated with index zero, no heat exchange occurs in the steady state. This is due to the uniform temperature of the closed cylindrical surface surrounding the system's centre. The first computational model zone with index 1 (Fig. 1) is a hollow conductor conducting direct current. The second zone represents a slot filled with gas. According to previous assumptions, the slot was replaced by a solid body with an equivalent thermal conductivity  $\lambda_2$ , which consists of a convective and radiation part [8],[9],[10]. The third model zone is a metallic enclosure. The fourth (last) zone represents a thin insulation that covers the above-mentioned enclosure. It is assumed in the subsequent analysis that the length of the system (Fig. 1) is much greater than its diameter ( $l \gg 2R_5$ ). Moreover, it is assumed that the system is positioned horizontally and is shielded from solar radiation. A constant ambient temperature  $T_a$  is also assumed. A constant value of the total heat transfer coefficient  $\alpha$  on the system's outer surface ( $r=R_5$ ) is assumed, where  $\alpha$  is the sum of the convective and the radiation coefficient. It follows from the aforementioned

simplifying assumptions that the stationary thermal field of the system can be approximated with the function of the radial coordinate,  $r$ .

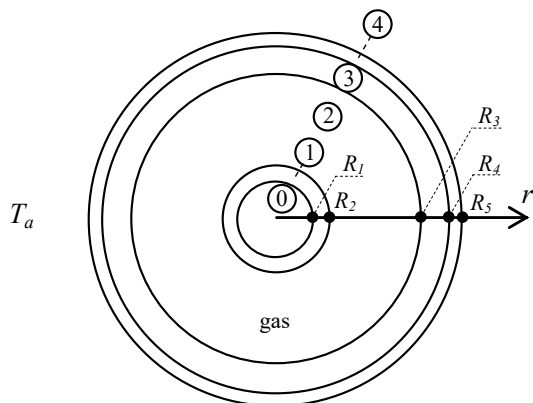


Fig. 1. Model of the direct current gas-insulated line

The mathematical model of the system is formulated with respect to increments  $v_i(r)$  related to ambient temperature  $T_a$

$$(1) \quad v_i(r) = T_i(r) - T_a$$

where  $T_i(r)$  denotes the distribution of temperature in the  $i$ -th zone.

With the adopted assumptions, the stationary temperature increment in the system is described by the classical heat equation (Poisson) [12,13] in the form:

$$(2) \quad \frac{1}{r} \frac{d}{dr} \left( r \frac{dv_i(r)}{dr} \right) = -\frac{g_i}{\lambda_i} \text{ for } R_i \leq r \leq R_{i+1} \text{ and } i=1,2,3,4,$$

where:  $\lambda_i$  is the thermal conductivity of the  $i$ -th zone,  $g_i=0$  for  $i=2,3,4$ . The efficiency of the heat source in the hollow conductor,  $g_1$ , is defined as below:

$$(3) \quad g_1 = g = \rho \frac{I^2}{\pi^2 (R_2^2 - R_1^2)^2},$$

where  $\rho$  is the averaged electric resistivity of the conductor, and  $I$  is the intensity of direct current flowing through the conductor.

As has been mentioned earlier, in the steady state in the zone designated with index zero, no heat exchange occurs. This implies an adiabatic boundary condition on the inner surface of the hollow conductor for  $r=R_1$

$$(4) \quad \left. \frac{dv_1(r)}{dr} \right|_{r=R_1} = 0.$$

It is assumed that on the outer surface of the system ( $r=R_5$ ) the exchange of heat with the environment occurs following the Newton law [14]. The above-mentioned exchange of energy is described by the boundary condition of the third kind (Hankel's).

$$(5) \quad \left. \frac{dv_4(r)}{dr} \right|_{r=R_5} = -\frac{\alpha}{\lambda_4} v_4(r=R_5),$$

where  $\alpha$  is the total heat transfer coefficient, which allows for both convection and radiation.

Individual model regions (Fig. 1) adjoin to each other. Therefore, the conditions of the continuity of temperature

and heat flux increment at the boundaries of the system's zones are satisfied

$$(6) \quad v_{i-1}(r=R_i) = v_i(r=R_i) \text{ for } i=2,3,4,$$

$$(7) \quad \lambda_{i-1} \left. \frac{dv_{i-1}(r)}{dr} \right|_{r=R_i} = \lambda_i \left. \frac{dv_i(r)}{dr} \right|_{r=R_i} \text{ for } i=2,3,4.$$

In order to determine the field distributions, relationship (2) was integrated twice. After considering that in the first zone  $g \neq 0$ , the following was obtained

$$(8) \quad v_1(r) = -\frac{gr^2}{4\lambda_1} + C_1 \ln r + C_2 \text{ for } R_1 \leq r \leq R_2$$

$$(9) \quad v_i(r) = C_{2i-1} \ln(r) + C_{2i} \text{ for } R_i \leq r \leq R_{i+1} \text{ and } i=2,3,4,$$

where:  $C_1, C_2, C_{2i-1}, C_{2i}$  - integration constants. To determine the above-mentioned constants, the following substitutions were made: (8) and (9) for  $i=2,3,4$  in (6-7), relationship (8) in (4) and relationship (9) for  $i=4$  in (5). This yielded a system of equations, which enabled the calculation of the constants in increments (8),(9). Finally, using relationship (1), the stationary distribution of temperature in all regions of the model was determined.

$$(10) \quad T_1(r) = T_a - \frac{g(r^2 - R_2^2)}{4\lambda_1} + \frac{gR_1^2}{2\lambda_1} \ln \frac{r}{R_2} + \frac{g(R_2^2 - R_1^2)}{2\lambda_2} \ln \frac{R_3}{R_2} + \frac{g(R_2^2 - R_1^2)}{2\lambda_3} \ln \frac{R_4}{R_3} + \frac{g(R_2^2 - R_1^2)}{2\lambda_4} \ln \frac{R_5}{R_4} + \frac{g(R_2^2 - R_1^2)}{2\alpha R_5}$$

for  $R_1 \leq r \leq R_2$ ,

$$(11) \quad T_2(r) = T_a - \frac{g(R_2^2 - R_1^2)}{2\lambda_2} \ln \frac{r}{R_3} + \frac{g(R_2^2 - R_1^2)}{2\lambda_3} \ln \frac{R_4}{R_3} + \frac{g(R_2^2 - R_1^2)}{2\lambda_4} \ln \frac{R_5}{R_4} + \frac{g(R_2^2 - R_1^2)}{2\alpha R_5}$$

for  $R_2 \leq r \leq R_3$ ,

$$(12) \quad T_3(r) = T_a - \frac{g(R_2^2 - R_1^2)}{2\lambda_3} \ln \frac{r}{R_4} + \frac{g(R_2^2 - R_1^2)}{2\lambda_4} \ln \frac{R_5}{R_4} + \frac{g(R_2^2 - R_1^2)}{2\alpha R_5}$$

for  $R_3 \leq r \leq R_4$ ,

$$(13) \quad T_4(r) = T_a - \frac{g(R_2^2 - R_1^2)}{2\lambda_4} \ln \frac{r}{R_5} + \frac{g(R_2^2 - R_1^2)}{2\alpha R_5}$$

for  $R_4 \leq r \leq R_5$ .

Associated with the thermal field is the steady-state current rating,  $I_{cr}$ . This is the maximum value of current, for which the temperature of the conductor ( $r=R_1$ ) may not exceed the maximum sustained temperature,  $T_{max}$ , allowed for stand-off insulators and power connections

$$(14) \quad T_1(r=R_1, I=I_{cr}) = T_{max}.$$

In formula (10),  $r=R_1$  and relationship (3) were substituted. From (14), after transformations, the following was obtained

$$(15) \quad I_{cr} = \sqrt{\frac{(T_{max} - T_a)}{M}}, \text{ where}$$

$$(16) \quad M = \frac{\rho}{2\pi^2 \alpha R_5 (R_2^2 - R_1^2)} + \frac{\rho}{4\pi^2 \lambda_1 (R_2^2 - R_1^2)} - \frac{\rho R_1^2 \ln \frac{R_2}{R_1}}{2\pi^2 \lambda_4 (R_2^2 - R_1^2)^2} + \frac{\rho \ln \frac{R_3}{R_2}}{2\pi^2 \lambda_2 (R_2^2 - R_1^2)} + \frac{\rho \ln \frac{R_4}{R_3}}{2\pi^2 \lambda_3 (R_2^2 - R_1^2)} + \frac{\rho \ln \frac{R_5}{R_4}}{2\pi^2 \lambda_4 (R_2^2 - R_1^2)}.$$

Formulas (15) and (16) define the steady-state current rating as a function of many parameters.

### Computation examples

A program has been developed in the Mathematica 11.1 environment [15], which determines the distributions of temperature based on relationships (10)-(13) and computes the steady-state current rating using formulas (15),(16). As an example, a GIL system was analyzed, which was made up of an aluminium hollow conductor and an aluminium enclosure.

For the computation of the equivalent thermal conductivity of a gas (filling the slot), the knowledge of the gas parameters is necessary. Parameters, e.g. for air, are given in [8]. The possibility of introducing the equivalent thermal conductivity of the gas,  $\lambda_2$ , (for the cylindrical slot under consideration) depends on the Rayleigh number criterion ( $Ra$ ). For  $T \leq 90^\circ C$  it occurs that  $Ra \leq 5.6 \cdot 10^6$  and thus  $Ra$  is less than the permissible value  $10^7$ . Therefore, the convective part of the equivalent thermal conductivity was calculated from the relationship provided in [8] (formulas 9.59-9.60). In turn, the radiation part was determined based on relationships given in [9] (formula 10.37), where the following values of the emissivity of the surfaces surrounding the slot were taken for computation:  $\varepsilon_1 = \varepsilon_3 = 0.95$ . The total heat transfer coefficient  $\alpha$  outside the system ( $r > R_5$ ) was calculated using the appropriate characteristic numbers [8], taking into account the geometrical dimensions of the system. Ultimately, the following data were used for computations:

$$(17) \quad R_1=0.0762 \text{ m}, \lambda_1=200 \text{ W/(mK)}, R_2=0.0889 \text{ m}, \lambda_2=0.522 \text{ W/(mK)}, R_3=0.33 \text{ m}, \lambda_3=200 \text{ W/(mK)}, R_4=0.338 \text{ m}, \lambda_4=0.17 \text{ W/(mK)}, R_5=0.341 \text{ m}, \rho(T=90^\circ C)=3.6234 \cdot 10^{-8} \Omega m, T_a=20^\circ C, \alpha=8.24 \text{ W/(m}^2 K).$$

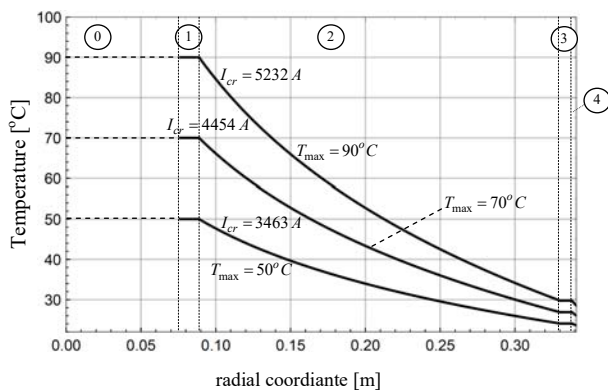


Fig. 2. Distributions of temperature in all zones of the direct current gas-insulated line

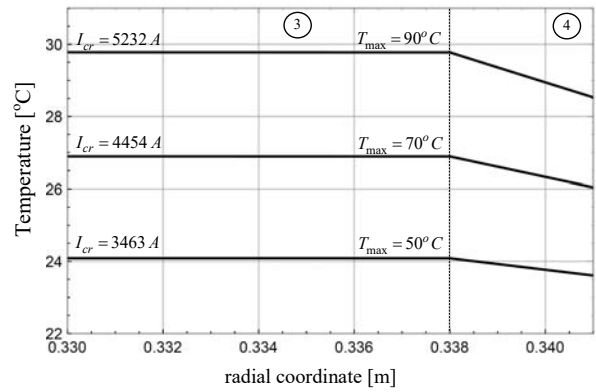


Fig. 3. Distribution of temperature, respectively, in the third and the fourth zones of the direct current gas-insulated line

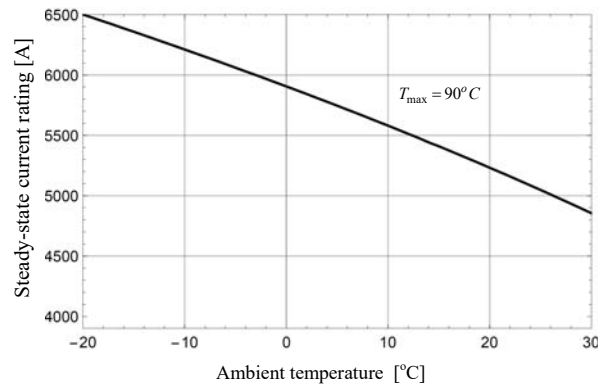


Fig. 4. Relationship of the steady-state current rating as a function of ambient temperature

The results of field distribution computations are presented graphically. Figure 2 shows the distributions of temperature in all regions of the direct current gas-insulated line for three values of the maximum sustained temperature:  $T_{max}=90^\circ C$ ,  $70^\circ C$ , and  $50^\circ C$ . To improve the legibility of Fig.2, the distributions in the third and the fourth model zones were shown separately in Fig. 3. In turn, Fig. 4 illustrates the dependence of the steady-state current rating on ambient temperature,  $T_a$ . When computing the aforementioned current, the heat transfer coefficient was determined for each ambient temperature  $T_a$  separately. This was due to a large change in the temperature of the system's outer surface with the change in ambient temperature  $T_a$ .

### Concluding remarks

From the performed analysis, the following conclusions are drawn:

- In the hollow conductor ( $r \in \langle R_1, R_2 \rangle$ ) and in the enclosure ( $r \in \langle R_3, R_4 \rangle$ ), the thermal field is almost uniform and does not depend on the radial coordinate,  $r$ . This is due to the large value of the thermal conductivity of aluminium ( $\lambda_1 = \lambda_3$ ), i.e. the small value of the Biot number. In turn, significant drops in temperature with the increase in  $r$  are observed in the gas ( $r \in \langle R_2, R_3 \rangle$ ) and in the outer insulation ( $r \in \langle R_4, R_5 \rangle$ ) (Fig. 2, Fig. 3). The cause of this phenomenon are very small values of  $\lambda_2$  and  $\lambda_4$ , compared to  $\lambda_1 = \lambda_3$ .
- The significant change in maximum sustained temperature  $T_{max}$  has little effect on the temperature of the system's outer surface  $T_4(r=R_5)$ . For instance, for

$T_{\max} \in \langle 50^{\circ}C, 90^{\circ}C \rangle$  the following is true:

$T_4(r=R_5) \in \langle 23.61^{\circ}C, 28.53^{\circ}C \rangle$  (Fig. 2, Fig. 3).

C) For  $T_{\max}=90^{\circ}C$ , not only stand off insulators and power connections are safe. In addition, the relationships  $T_4(r=R_4)=29.78^{\circ}C < 70^{\circ}C$  and  $T_4(r=R_5)=28.53^{\circ}C < 40^{\circ}C$  are true (Fig. 3). The first inequality provides the thermal safety of the outer insulation, while the second, of the environment.

D) The increase in the maximum sustained temperature  $T_{\max}$  causes a substantial increase in steady-state current rating  $I_{cr}$  (Fig. 2, Fig. 3). For example, the following implication is true:

$T_{\max} \in \langle 50^{\circ}C, 90^{\circ}C \rangle \Rightarrow I_{cr} \in \langle 3463 A, 5232 A \rangle$ . In turn, the increase in ambient temperature  $T_a$  results in a decrease in  $I_{cr}$  (Fig. 4). The first statement is obvious, while the second is due to a worsening in the cooling conditions of the DC GIL system.

The above remarks show that the presented solution has a very good physical interpretation.

#### ACKNOWLEDGEMENT

The paper was prepared at Białystok University of Technology within a framework of the WZ/WE-IA/7/2023 project funded by Ministry of Education and Science, Poland

**Authors:** prof. J. Gołębiowski<sup>1</sup>, D.Sc., Ph.D., M. Zaręba<sup>2</sup>, Ph.D., Białystok University of Technology, Faculty of Electrical Engineering, 15-351 Białystok, 45 D Wiejska Street, Poland, e-mail: <sup>1</sup>j.golebiowski@pb.edu.pl, <sup>2</sup>m.zareba@pb.edu.pl

#### REFERENCES

- [1] Magier T., Tenzer M., Koch H., Direct current gas-insulated transmission lines, *IEEE Trans. Power. Deliv.*, 33 (2018), No. 1, 440-446.
- [2] Ma J., Zhang Q., Wu Z., Guo C., Wen T., Liu L., Influence of operating voltage on breakdown characteristics of HVDC GIL under impulse voltage, *12th International Conference on the Properties and Applications of Dielectric Materials (ICPADM)*, Xi'an, China, 1006-1009, (2018).
- [3] Szczegielniak T., Kusiak D., Jabłoński P., Determination of the operating temperature of the gas-insulated transmission line, *Appl. Sci.*, 10 (2022), No. 24, 8877.
- [4] Kim J.K., Hahn S.C., Park K.Y., Kim H.K., Oh Y.H., Temperature rise prediction of EHV GIS bus bar by coupled magnothermal finite element method, *IEEE Trans. Magn.*, 41 (2005), No. 5, 1636-1639.
- [5] Kim S.W., Kim H.H., Hahn S.C., Lee B.Y., Park K.Y., Shin Y.J., Song W.P., Kim J.B., Shin I.H., Coupled finite-element-analytic technique for prediction on temperature rise in power apparatus, *IEEE Trans. Magn.*, 38 (2002), No. 2, 921-924.
- [6] Kim H.K., Oh Y.H., Lee S.H., Calculation of temperature rise in gas insulated busbar by coupled magneto-thermal-fluid analysis, *J. Electr. Eng. Technol.*, 4 (2009), No. 4, 510-514.
- [7] Nawrowski R., Tory wielkopiędowe izolowane powietrzem lub SF<sub>6</sub> (Air-insulated or SF<sub>6</sub> high current busbars), *Oficyna Wydawnicza Politechniki Poznańskiej*, Poznań (1998).
- [8] Incropera F., Witt D. De., Bergman T., Lavine A., Introduction to heat transfer, *John Wiley and Sons*, USA (2007).
- [9] Pieńkowski C.A., Przepływ ciepła i wymienniki (Heat flow and exchangers), *Wydawnictwo Politechniki Białostockiej*, Białystok (2007).
- [10] Wiśniewski S., Wymiana ciepła (Heat exchange), *Wydawnictwo Naukowo Techniczne*, Warszawa (2017).
- [11] Li B., Gu T., Li B., Zhang Y., Study on the gas-insulated line equivalent model and simplified model, *Energies*, 10(2017), No. 7, 901.
- [12] Latif M.J., Heat conduction, *Springer-Verlag*, Berlin, Haidelberg (2009).
- [13] Baehr M. D., Stephan K., Heat and mass transfer, *Springer-Verlag*, Berlin, Heidelberg (2006).
- [14] Hering M., Termokinetyka dla elektryków (Thermokinetics for electricians), *Wydawnictwo Naukowo Techniczne*, Warszawa (1980).
- [15] Wolfram Research Inc., Mathematica, *Champaign*, Illinois (2022).